

Regulation of cyclic and linear electron flow in higher plants

Pierre Joliot^{a,1} and Giles N. Johnson^b

^aInstitut de Biologie Physico-Chimique, Unité Mixte de Recherche 7141, Centre National de la Recherche Scientifique and Université Pierre et Marie Curie-Université Paris 6, 75005 Paris, France; and ^bFaculty of Life Sciences, University of Manchester, Manchester M13 9PT, United Kingdom

Contributed by Pierre A. Joliot, June 27, 2011 (sent for review May 3, 2011)

Cyclic electron flow is increasingly recognized as being essential in plant growth, generating a pH gradient across thylakoid membrane (ΔpH) that contributes to ATP synthesis and triggers the protective process of nonphotochemical quenching (NPQ) under stress conditions. Here, we report experiments demonstrating the importance of that ΔpH in protecting plants from stress and relating to the regulation of cyclic relative to linear flow. In leaves infiltrated with low concentrations of nigericin, which dissipates the ΔpH without significantly affecting the potential gradient, thereby maintaining ATP synthesis, the extent of NPQ was markedly lower, reflecting the lower ΔpH . At the same time, the photosystem (PS) I primary donor P700 was largely reduced in the light, in contrast to control conditions where increasing light progressively oxidized P700, due to down-regulation of the cytochrome *bf* complex. Illumination of nigericin-infiltrated leaves resulted in photoinhibition of PSII but also, more markedly, of PSI. Plants lacking ferredoxin (Fd) NADP oxidoreductase (FNR) or the polypeptide proton gradient regulation 5 (PGR5) also show reduction of P700 in the light and increased sensitivity to PSI photoinhibition, demonstrating that the regulation of the cytochrome *bf* complex (*cyt bf*) is essential for protection of PSI from light stress. The formation of a ΔpH is concluded to be essential to that regulation, with cyclic electron flow playing a vital, previously poorly appreciated role in this protective process. Examination of cyclic electron flow in plants with a reduced content of FNR shows that these antisense plants are less able to maintain a steady rate of this pathway. This reduction is suggested to reflect a change in the distribution of FNR from cyclic to linear flow, likely reflecting the formation or disassembly of FNR–cytochrome *bf* complex.

photosynthesis | photoprotection | electron transport

Plants have developed a complex set of mechanisms to adapt the photosynthetic process, in particular the flow of electrons into and through the electron transport chain, to changes in light intensity, which varies naturally by orders of magnitude ranging from seconds to months. Photosynthetic electron transport can operate in two modes. In the linear mode, electrons are transferred from water to NADP via three major transmembrane complexes: Photosystem II (PSII), the cytochrome *b₆f* complex (*cyt bf*), and photosystem I (PSI). NADPH so produced is used in the Calvin-Benson-Bassham cycle, where CO₂ is fixed to produce sugars. Cyclic electron transfer involves only PSI and *cyt bf* and was first described by Arnon (1). It involves electron flow to generate an electrochemical proton gradient across the thylakoid membrane without net production of reducing equivalents. In recent years, both the role and the regulation of cyclic electron flow have been widely debated; for reviews see refs. 2–5.

It is known that most PSII reaction centers are localized in the appressed region of the thylakoid membrane, within the grana stacks (6, 7) and that diffusion of plastoquinone (PQ) is restricted to small membrane domains, including a few PSII centers (8–10). Consequently, PQH₂ generated by PSII can only be reoxidized by that fraction of *cyt bf* also localized in the appressed region ($\approx 47\%$) (6). It can be assumed that long-distance electron transfer between the appressed and nonappressed

regions is mediated by plastocyanin (PC). PSI, in contrast, is localized at the margins of the grana and in the nonappressed membranes. In higher plants, there is the potential for spatial separation of cyclic electron flow, in the nonappressed membranes, from linear flow, between PSII in the appressed membranes and PSI in the grana margins (5).

Two major functions for cyclic electron flow are presumed. (i) ATP synthesis: The stoichiometry of proton pumping and ATP synthesis have long been debated; however, a consensus has now emerged that linear electron transport alone probably generates insufficient ATP to balance the ATP:NADPH consumption of the Calvin-Benson-Bassham cycle (3, 4, 11). The shortfall is probably supplied by cyclic electron flow. At the onset of illumination of a dark adapted leaf, there is a rapid light-induced formation of ATP (12) which is obligatorily associated with the occurrence of a cyclic process. (ii) Control of light harvesting: Under strong illumination, cyclic electron flow increases, generating a large proton gradient required for the formation of nonphotochemical quenching (NPQ) within the antenna, protecting PSII against excess light (13–15).

Illumination under strong light also induces the oxidation of a large fraction of P700 (16–18). Under high light conditions, overall photosynthesis is limited at the level of the Calvin-Benson-Bassham cycle and all electron carriers localized before this cycle should be in a reduced state. Thus, the observation that P700 becomes oxidized under strong light demonstrates that some regulatory process must limit the rate of electron flow before P700. Measurements of the redox state of multiple components of the electron transport chain demonstrate that this regulation occurs at the level of the *cyt bf*, probably at the step of plastoquinol oxidation. It has long been recognized that this reaction is sensitive to the pH of the thylakoid lumen (19) and so the generation of a pH gradient may lead to a slowing of electron flow through the *cyt bf* complex. Johnson (20) presented evidence that the *cyt bf* is also sensitive to redox poise in the physiologically relevant range, and work from Hald et al. (21) led to the proposal that it is specifically the redox poise of the NADP/H pool that is responsible for regulation of *cyt bf* in vivo. Regulation of electron transport before PSI prevents the over-reduction of Fe-S centers on the PSI acceptor side capable of reducing oxygen to superoxide. Furthermore, PSI centers including P700⁺ are efficient nonphotochemical quenchers that protect the nonappressed region of the membrane against excess light. Regulation of the *cyt bf* complex therefore plays a substantial and previously underappreciated role in protecting plants from oxidative stress.

The mechanism of cyclic electron flow remains a subject of controversy. Several pathways have been proposed: (i) Electrons

Author contributions: P.J. and G.N.J. designed research, performed research, analyzed data, and wrote the paper.

The authors declare no conflict of interest.

¹To whom correspondence should be addressed. E-mail: pierre.joliot@ibpc.fr.

This article contains supporting information online at www.pnas.org/lookup/suppl/doi:10.1073/pnas.1110189108/-DCSupplemental.

are transferred to plastoquinone via a plastoquinone reductase (NDH) homologous to mitochondrial complex I. The low concentration of NDH present in the membrane (22) is not compatible with the large rate of cyclic electron flow ($>100 \text{ s}^{-1}$) (23, 24). Also, it is evident that plants lacking the NDH complex are still capable of cyclic electron flow. Nevertheless, under weak light, a significant cyclic flow could be mediated by NDH. (ii) Electrons are transferred from ferredoxin (Fd) to plastoquinone via a putative ferredoxin-quinone reductase (FQR) (25, 26). FQR should be present at a high concentration but has never been identified through biochemical or genetic approaches. (iii) Electrons are passed from ferredoxin to the cyt *bf* complex and from there to plastoquinone, in agreement with earlier observations that ferredoxin is capable of mediating cyclic flow in isolated thylakoids (1). We previously proposed a mechanistic model in which cyclic electron flow operates according to a Q-cycle process (4, 24) similar to that initially proposed by Mitchell (27). The concerted transfer of two electrons from Fd and cyt *b_L* to PQ at site Q_i leads the formation of PQH₂, which is then rapidly reoxidized at site Q_o. This Q-cycle process differs from the modified Q cycle (28) in which the reduction of PQ at site Q_i requires the sequential transfer of two electrons from the cyt *b* chain. In our model, the modified Q cycle operates in cyt *bf* centers in the appressed region of the thylakoid, which are involved in the oxidation of PQH₂ generated by PSII.

Clark et al. (29) and Zhang et al. (30) have isolated and purified complexes in which Fd-NADP reductase (FNR) is associated with cyt *bf* and it has widely been discussed that this may mediate ferredoxin binding and/or electron transfer through the cyclic pathway. In the alga *Chlamydomonas*, supercomplexes involving PSI and cyt *bf* were first observed by Wollman and Bulté (31) and more recently, Iwai and colleagues have purified functional complexes also involving FNR and a peptide termed PGRL1 (32). Proton gradient regulation like 1 (PGRL1) is an intrinsic membrane peptide, first identified in *Arabidopsis*, where it is thought to anchor a second peptide, PGR5 to the membrane. Mutants lacking either PGR5 (33) or PGRL (34) are impaired in, but not incapable of, cyclic electron flow (34, 35). DalCorso et al. (34) used yeast two-hybrid assays to show evidence for interactions of PGRL1 with PSI, Fd, FNR, and cyt *bf*. Moreover, PGRL copurifies with PSI. These observations led these authors to propose the formation of supercomplexes including these proteins, possibly including a putative additional FQR protein; these supercomplexes would be involved in the switch between linear and cyclic electron flow. Regardless of the presence of supercomplexes, it remains likely that FNR is required for cyclic electron flow and that the partitioning of this between cyt *bf*-bound and soluble pools may play a role in regulating electron transport processes. In this paper, we consider different possible arrangements of the electron transfer chain: In the linear configuration, we suggest that FNR is not bound to cyt

bf and electrons are preferentially transferred from Fd to NADP. In the cyclic configuration, we propose, as a working hypothesis, that association of FNR with cyt *bf* creates a binding site for Fd, allowing electron transfer to the Q_i site of cyt *bf* (Fig. 1). Alternatively, supercomplexes may form, including PSI, cyt *bf*, and FNR, similar to those proposed by DalCorso et al. (34) and isolated from *Chlamydomonas* by Iwai et al. (32).

Here, the efficiency of the cyclic process in generating a proton gradient that protects the chloroplasts against excess light is examined in different conditions (presence of nigericin, plants with reduced FNR level or plants lacking *pgr5*) and data are discussed in the light of the models described above. We also examine the regulation of the cyt *bf* complex and how that regulation interacts with cyclic electron flow.

Results and Discussion

In Fig. 2*A* and *B*, chlorophyll fluorescence parameters are shown during the first minutes of illumination of a dark-adapted *Arabidopsis* leaf, in the presence or absence of 0.5 μM nigericin, a proton/potassium ion exchanger that specifically collapses the transmembrane proton gradient while maintaining an electrochemical gradient. At this low concentration of nigericin, no significant effect could be observed on the rate of electron flow through PSII; however, a substantial effect was seen on NPQ. ATP synthesis is driven by the electrochemical potential gradient across the thylakoid membrane, whereas NPQ depends simply on proton concentration in the lumen. Nigericin lowers the latter but maintains the electrical gradient; thus, we conclude that a sufficient potential gradient is maintained to produce sufficient ATP for CO₂ fixation. Inhibiting NPQ will increase energy transfer to the PSII reaction centers; however, under the conditions here, where electron flow is limited downstream of PSII, this does not result in any change in Φ_{PSII} . Examination of the relaxation of NPQ following the cessation of illumination (Fig. S1) demonstrates that this relaxation is accelerated in the presence of nigericin, implying that the low level of quenching seen is due to pH-dependent quenching (qE) rather than photo-inhibition of PSII (qI) (36, 37). In Fig. 2*C*, the proportion of P700 in the oxidized state is shown, measured under the same conditions in a separate leaf from the same plant. This was determined by interrupting illumination for 200 ms at the time indicated by the points (Fig. S2). In the absence of nigericin, P700 becomes progressively more oxidized. In the presence of nigericin, only a small proportion of P700 was observed as being oxidized ($\approx 15\%$ of total pool) with this proportion remaining nearly constant throughout the period of illumination. This suggests that acidification of the lumen affects both NPQ formation and oxidation of P700. Given that both NPQ and regulation of the flow of electrons are predicted to have a protective effect against light stress, we expect that addition of nigericin will result in increased photodamage to both reaction centers. We

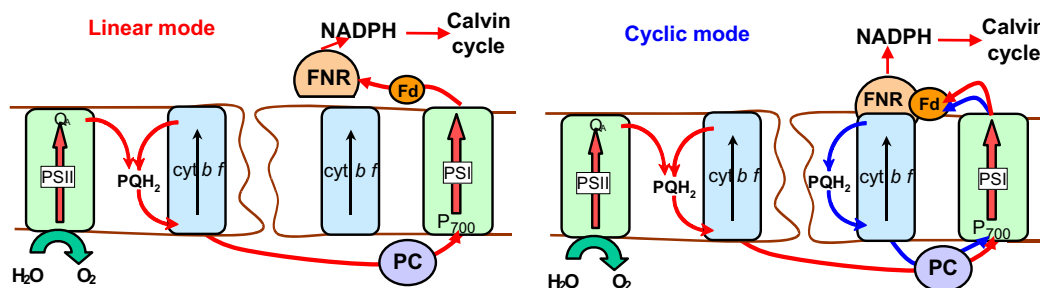


Fig. 1. Model for structural organization of the photosynthetic chain in the linear (Left) and cyclic (Right) configuration.

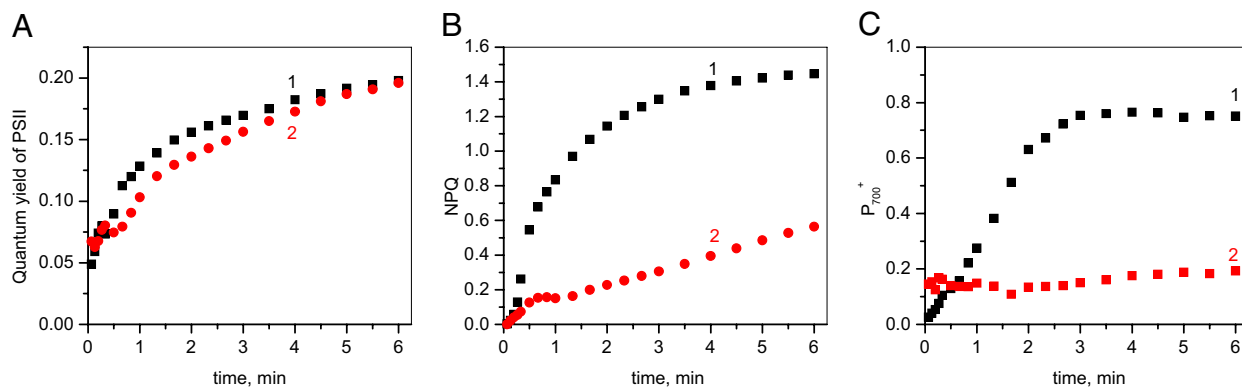


Fig. 2. Effect of nigericin on the kinetics of PSII quantum yield (A), NPQ formation (B), and oxidation of P700 (C) measured during the course of a 6-min illumination of wild-type *Arabidopsis* leaves. In the following, we express the light intensity as a photochemical rate constant, i.e., the number of photons absorbed per reaction centers and per second determined on the basis of membrane potential measurements (40). On this basis, the turnover rate of PSI and PSII reactions can be computed by multiplying the photochemical rate constant by the quantum yield. Illumination was provided in the form of a green light ($\lambda_{\text{max}} = 530$): $\text{kiPSII} \approx \text{kiPSII} \approx 200 \text{ s}^{-1}$ or $400 \mu\text{mol photons m}^{-2} \text{ s}^{-1}$). The leaf was vacuum infiltrated with a solution containing 150 mM sorbitol with (red circles) or without (black squares) 0.5 μM nigericin. A total of 330 mM sorbitol was included to avoid osmotic shock.

measured the fraction of PSI centers irreversibly inactivated following intense illumination of *Arabidopsis* leaves. In the presence of 2 μM nigericin, preventing most ΔpH formation, a 20-min illumination resulted in an inactivation of 69% of PSI and 29% of PSII centers (Table S1). Previously, Johnson and Ruban (38) observed that in the presence of 50 μM nigericin, a large NPQ was formed, which does not relax in the dark. This NPQ is associated with an irreversible inhibition of a large fraction of PSII centers. We thus conclude that acidification of lumen plays a key role in the protection of both the PSI and the PSII against light excess and that PSI is actually more vulnerable to photodamage than PSII under conditions where the cyt bf complex is not regulated.

Hald et al. (21) examined the level of P700 oxidation across a range of light intensities in tobacco wild type and in two antisense mutants partially depleted in the enzymes FNR, which oxidizes ferredoxin and reduces NADP or in glyceraldehyde-3-phosphate dehydrogenase (GAPDH), the principal consumer of NADPH. FNR-depleted mutants showed extensive bleaching when grown under moderate light and across a range of irradiances, had little or no oxidation of P700 under steady-state conditions. In this respect, their behavior was similar to that of plants infiltrated with nigericin. In contrast, plants lacking GAPDH, where there was a similar degree of inhibition of photosynthesis, showed little bleaching and no evidence of oxi-

dativ stress. In antisense (as)-GAPDH plants, the level of P700 oxidation was slightly higher than in the wild type and the apparent rate constant for P700 reduction following illumination was approximately half that in the wild type, implying a lower turnover rate of the cyt bf complex. These experiments were interpreted as showing that cyt bf turnover is controlled in response to the fraction of reduced NADPH, which tends to be high in GAPDH-depleted plants but low in FNR-depleted mutants (21). Relating to our working hypothesis (Fig. 1) we propose that the formation of an FNR-cyt bf complex (cyclic configuration) might be triggered by the reduction of the NADP pool and the dissociation of the complex by the oxidation of the NADPH pool (linear configuration). We have compared the quantum yield of PSII, NPQ, and the level of oxidation of P700 during the course of illumination of a tobacco wild type and on an antisense mutant partially depleted in FNR (as-FNR). In Fig. 3, leaves were illuminated for 8 min under green light ($\text{kiPSI} \approx \text{kiPSII} \approx 200 \text{ s}^{-1}$). The steady state quantum yield of PSII in as-FNR was about half that measured on the wild type, indicating the extent of inhibition of linear electron flow. Apart from during the first 4 s of illumination, the rate of PSII turnover was found to be inhibited in as-FNR plants to a similar degree throughout the induction period. This implies that FNR represents a limitation on electron transport throughout the induction of photosynthesis, even though the ultimate limiting factor for electron

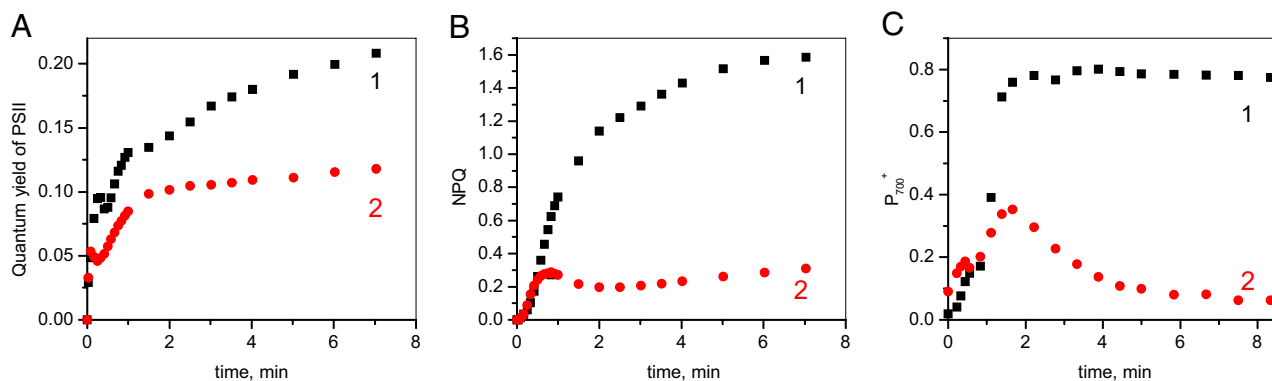


Fig. 3. Changes in PSII quantum yield (A), NPQ formation (B), and oxidation of P700 (C) measured during the course of 8 min of illumination under green light (intensity $\text{kiPSI} \approx \text{kiPSII} \approx 200 \text{ s}^{-1}$) of dark-adapted wild type (black squares) and as-FNR (red circles) tobacco leaves. Wild type: $F_v/F_{\text{max}} = 0.82$. As-FNR mutant: $F_v/F_{\text{max}} = 0.85$.

transport during induction is CO₂ fixation. Fig. 3B displays the kinetics of NPQ formation measured at the same time as PSII efficiency. In the wild type, there is a progressive rise in NPQ through time, with a plateau being reached after 8 min of illumination. In the as-FNR plants, the initial induction of NPQ is similar to that observed in the wild type, whereas at 8 min, the NPQ level is approximately five times lower than for the wild type. Our results contrast with the observations of Hald et al. (21) who observed little inhibition of reversible NPQ under steady-state conditions. This difference in behavior may reflect differences in growth conditions. In the wild type, most NPQ relaxes rapidly after 1- and 8-min illuminations, respectively (Fig. S3). This relaxation reflects the decay of pH gradient formed during the illumination. In the mutant, a fast NPQ relaxation (completed in 1 min) is observed after a 1-min illumination, whereas after 8 min, only a small fraction relaxes in a time range of 4 min. This experiment suggests that, under the conditions used here, there is a shift during induction in the type of NPQ in the mutant toward one that does not readily relax in the dark. A likely hypothesis is that illumination induces an inhibition of the PSII electron donors, which leads to formation of inactive PSII centers blocked in a quenching state. In Fig. 3C, the proportion of reversibly oxidized P700 is shown as a function of illumination time in a similar leaf. In the wild type, a maximum level of P700 oxidation (≈ 0.8) is reached after ≈ 5 min of illumination. In the case of the FNR antisense plants, an initial peak of P700 oxidation is followed by a rereduction, giving a low stationary level of oxidation of P700 (0.04). Under the conditions used here, plants lacking FNR failed to maintain a substantial ΔpH at steady state and also failed to accumulate oxidized P700. Nevertheless, there was evidence for the induction of a transient ΔpH , sufficient to induce a low level of reversible NPQ. This peak in ΔpH coincided with a transient peak in P700 oxidation in the mutant (compare Fig. 3B to 3C). However, a low P700⁺ concentration (0.08) and a low level of pH-dependent NPQ was measured after a 25-min illumination. We suggest that during the first minute of illumination, the NADP pool becomes rapidly

reduced, which induces the association of most of the available FNR with cyt bf, leading to an efficient cyclic electron flow. Induction of CO₂ fixation oxidizes NADPH, inducing a dissociation of the FNR cyt bf complexes and therefore a switch from cyclic to linear flow. In Fig. 4A, cyclic electron flow in an *Arabidopsis* leaf is shown, using a procedure described in refs. 39, 40, in which P700 oxidation is analyzed under weak far-red light, which preferentially excites PSI. Leaves were illuminated for 5 min under far-red light ($kiPSI \approx 10 \text{ s}^{-1}$). In the black curve, the light is switched off for 1 min, a period of time sufficient to reduce cyt f, the Rieske protein, PC and P700 (about five electron equivalents), whereas the PQ pool remains oxidized. Illumination of the leaf under the same far-red light induces a fast oxidation of P700, similar to that observed in dark-adapted leaves in the presence of the PSI electron acceptor methyl viologen, which prevents the occurrence of cyclic electron flow (39). We thus conclude that, in these conditions, electron transport operates in the linear mode. In the following curves, the leaf was illuminated by pulses of saturating light of various durations superimposed on the far-red light. At the end of the saturating pulse, all light was switched off for 2 s before far-red light was reapplied. The period of 2-s darkness is sufficient to reduce P700⁺ and to oxidize most of the PSI acceptors (23). For pulses between 20-ms and 2-s duration, the kinetics of PSI donor oxidation displays a lag phase of increasing duration as function of the duration of the pulses. We ascribe this lag phase to the time necessary to oxidize the fraction of the PQ pool that was reduced during the light pulse. A lag phase of maximum duration is observed after a 200-ms pulse, corresponding to the time necessary to fully reduce all of the PSI donors, including PQ, and the PSI acceptors, as independently judged from fluorescence experiments (41, 42). The duration of the lag in P700 oxidation is ≈ 1.1 s and the number of electrons transferred during this lag phase is $1.1 \times 10^{-1} = 11$. This is in good agreement with the size of the PQ pool expressed as a number of electron equivalents (≈ 12 electrons). Following the lag phase, the kinetics of P700 oxidation is similar to that observed in curve 1 and reflects the oxi-

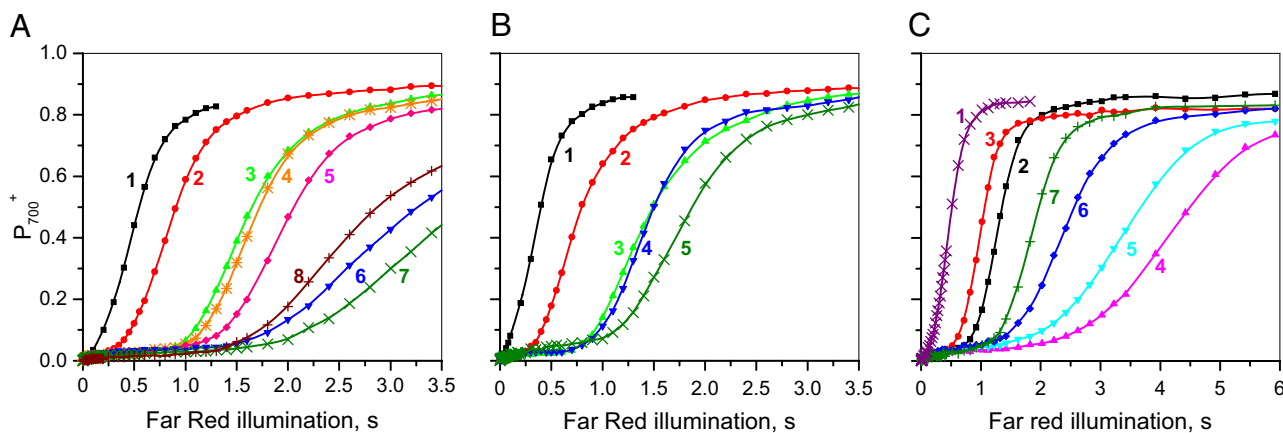


Fig. 4. (A and B) Comparison of the kinetics of P700 oxidation measured under weak far-red excitation ($kiPSI \approx 10 \text{ s}^{-1}$) of *Arabidopsis* wild type (A) and mutant lacking PGR5 (B). Black curves (curve 1 in A and B): leaves were preilluminated for 5 min of far-red light then darkened for 1 min before far-red illumination was reapplied. P700⁺ concentration is normalized to the maximum P700⁺, which was estimated by giving a 3-ms pulse of saturating light at the end of 8-s of far-red illumination. For the following curves, the leaves were exposed to pulses of saturating red light superimposed on the far-red excitation. Leaves were then transferred to darkness for 2 s before far-red light was reapplied. To obtain reproducible results, the leaf was illuminated for 5 min under far-red light between each experiment. Duration of the pulse: (A) curve 2, 20 ms; curve 3, 200 ms; curve 4, 2 s; curve 5, s; curve 6, 10 s; curve 7, 20 s; and curve 8, 30 s. (B) Curve 2, 20 ms; curve 3, 200 ms; curve 4, 10 s; and curve 5, 5 s. No further slow down is observed for pulses longer than 20 s. (C) Kinetics of P700 oxidation measured on an *Arabidopsis* leaf as a function of the time of dark following pulses of saturating light. Before each experiment, the leaf was illuminated for more than 5 min in far-red light. Curve 1 is the same as curve 1 in Fig. 3. In curves 2 and 3, a pulse of saturating light (200-ms duration) was superimposed on the far-red light, which was then switched off at the end of the pulse. Far-red excitation was reapplied after 2 s (curve 2) or 60 s (curve 3) of dark. In curves 4–8, a pulse of 15 s of red light was superimposed on the far-red light. Kinetics of P700 oxidation was measured after 2 s (curve 4) 4 s (curve 5), 10 s (curve 6), and 20 s (curve 7) of dark.

dation of the primary and secondary PSI donors (approximately five electron equivalents). Increasing the duration of the saturating pulse from 200 ms to 2 s does not induce a significant slowing down of P700 oxidation, showing that electrons are transferred to the Calvin-Benson-Bassham cycle or to oxygen via the Mehler reaction (linear mode). For longer times of illumination, the kinetics of P700 oxidation becomes progressively slower. The slowest P700 oxidation is observed after a 20-s pulse and, for longer pulses (30 s), the efficiency of cyclic flow decreases, with activation of the Calvin-Benson-Bassham cycle (39). The slowing of P700 oxidation was previously interpreted as reflecting an increasing fraction of the electrons on the acceptor side of PSI being transferred back to P700, thus reflecting a shift from linear to cyclic electron flow (39). An alternate hypothesis would be that the rate of P700 oxidation is limited by the oxidation of PSI acceptors. To test this hypothesis, P700 oxidation was measured under two far-red light intensities: $k_i\text{PSI} \approx 10 \text{ s}^{-1}$ and 48 s^{-1} (Fig. S4, curves 1 and 2, respectively) after a 15-s pulse of saturating light. A much faster kinetics of P700 oxidation was observed at the higher intensity, confirming that P700 oxidation is not limited by the reduction of PSI electron acceptors but probably by the rate of plastoquinol reduction that occurs at site Qo of the cyt bf complex.

Fig. 4B shows the same experiment performed on an *Arabidopsis* mutant lacking PGR5. For light pulses up to 2-s duration, essentially the same behavior is observed as in wild type. Increasing pulse length up to 10 s did not result in a further slowing of P700 oxidation, which only became marginally slower after a pulse of 20 s. This is consistent with previous observations, where it was concluded that, whereas the *pgr5* mutant is capable of cyclic electron flow, it is less readily switched into that mode. The implications of these results are that the induction of cyclic electron flow during the first seconds of light requires an activation step. Occurrence of cyclic flow implies that each reduced Fd formed on the acceptor side of PSI is transferred more rapidly to the cyt bf rather than to the free FNR involved in linear flow. This will occur if a large fraction of FNR is associated with cyt bf, to form complexes localized at a short distance from PSI (Fig. 1). Formation of these complexes might be facilitated by PGRL and PGR5, in agreement with a model proposed by DalCorso et al. (34).

In Fig. 4C the kinetics of P700 oxidation is shown as a function of the dark time between the saturating pulses and the far-red excitation. Curves 2 and 3 display the kinetics of P700 oxidation, measured 2 s and 60 s after a 200-ms pulse, respectively. The decrease in the duration of the lag phase as a function of the dark time reflects the slow oxidation of the PQ pool that occurs on a minute time scale. This experiment shows that the PQ pool stays largely reduced for 20 s after a short saturating illumination and hence it cannot be changes in the redox state of the PQ pool that give rise to the switch from linear to cyclic flow. Curves 4–7 show the kinetics of P700 oxidation measured after 2, 4, 10, and 20 s of dark, following a 15-s pulse of saturating light, sufficient to induce cyclic electron flow (Fig. 4). The acceleration of the kinetics as a function of the dark time reflects a progressive shift from a cyclic back to a linear mode in the dark ($t_{1/2} \approx 20 \text{ s}$). This slow relaxation may reflect a dissociation of the FNR cyt bf complexes (or supercomplexes, including PSI), which thus occurs in a similar time range to their formation.

The formation of ATP induced by the illumination of dark-adapted leaves can be estimated by measuring, in the dark, the electrochemical proton gradient (12) that is in thermodynamic equilibrium with the $[\text{ATP}]/[\text{ATP}] \times [P]$ ratio. Illumination of a leaf induces a long-lived (several minutes) $\Delta\mu\text{H}^+$ increase that reflects an increase in the ATP concentration with respect to that present in dark-adapted leaves, which is dependent upon respiratory activity (12). A large fraction of ATP is synthesized

during the first 30 s of illumination (figure 6 in ref. 12). This implies that at the onset of illumination, a large fraction of the protons pumped by the cyclic electron flow are consumed at the level of the ATP synthase for ATP synthesis.

Conclusions

In recent years, the importance of regulating the flow of electrons through the photosynthetic electron transport chain has increasingly been recognized as crucial to the health and survival of plants. Acidification of the lumen is shown here to play a crucial role in this regulation, preventing the light-induced inactivation (photoinhibition) of both PSI and PSII via the formation of nonphotochemical quenchers in the antenna of the appressed region and modulating the oxidation of P700 in the nonappressed region of the membrane. The former has been appreciated for a long time; however, the latter function is not so widely understood. Indeed, the precise details of how the cyt bf complex is regulated remain to be elucidated; however, an *in vivo* role of ΔpH in this process is clear. The regulation of the partitioning of electrons between the cyclic and linear pathways thus plays a key role in the adaptation of the plant to changes in the environment. The molecular processes occurring during this switch between linear and cyclic mode suggest some kind of activation step, such as the assembly/disassembly of a protein complex or even a supercomplex. The fact that plants with reduced levels of FNR and plants lacking PGR5 or PGRL have a reduced cyclic electron flow provides arguments that efficiency of the cyclic process is dependent upon the formation of complexes that include these three proteins associated with cyt bf. Under light-limiting conditions, most of FNR contributes to the linear electron flow process, whereas when the Calvin-Benson-Bassham cycle is rate limiting, reduction of the NADP pool induces the formation of FNR–cyt bf complexes that protect the appressed and nonappressed regions of the membrane against the excess of light via the cyclic process that induces the formation of a large proton gradient.

Methods

Plant Growth. Seeds of *Arabidopsis thaliana* expressing and lacking PGR5 were provided by T. Shikanai (Nara Institute of Science and Technology, Nara, Japan) (33). Seeds of tobacco wild type (variety Samson) and lacking FNR (FNR22) were provided by U. Sonnewald (Institut für Pflanzen-genetik und Kulturpflanzenforschung, Gatersleben, Germany) (43). *Arabidopsis* and wild-type tobacco were grown with a 14-h photoperiod at a light intensity of $50 \mu\text{mol photons m}^{-2} \text{ s}^{-1}$, temperature 20°C day, 16°C night. Plants of the FNR22 antisense line were grown at lower light intensity ($25 \mu\text{mol photons m}^{-2} \text{ s}^{-1}$) to limit photobleaching of the leaves.

Absorption Changes. Absorption changes were measured using a JTS spectrophotometer (Biologic) (24). The redox state of PSI donors was measured as changes in absorbance at 820 nm (44). At this wavelength, P700 and plastocyanin oxidation contribute 77 and 23% to the signal, respectively. In the text and figures, absorption changes at 820 nm are considered as giving an acceptable approximation of P700 redox state. Illumination was provided by LEDs peaking at 740 nm (far-red light), 540 nm (green light), or 620 nm (saturating red light) as indicated in the text. Because of the differences in absorption of these different wavelengths, irradiances are expressed as photochemical rate constants, rather than photon flux densities. Photochemical rate constants were estimated on the basis of measurements of membrane potential made at 520 nm, according to the method described in ref. 12.

Fluorescence. Fluorescence was measured using the JTS spectrophotometer. Fluorescence yield (F) is sampled using short detecting flashes (15- μs duration, 546 nm). The maximum fluorescence yield F_{max} is measured on dark adapted leaves. The fluorescence yield F_m is measured at the end of a 200-ms saturating light pulse superimposed to a continuous illumination. The saturating light pulse induces a full reduction of the primary PSII acceptor. The PSII quantum yield was calculated according to Genty et al. (45) as: $(F_m - F)/F_m$. NPQ was estimated as: $(F_{\text{max}} - F_m)/F_m$ (46).

1. Arnon DI, Allen MB, Whatley FR (1954) Photosynthesis by isolated chloroplasts. *Nature* 174:394–396.
2. Heber U (2002) Irrungen, Wirrungen? The Mehler reaction in relation to cyclic electron transport in C3 plants. *Photosynth Res* 73:223–231.
3. Allen JF (2003) Cyclic, pseudocyclic and noncyclic photophosphorylation: New links in the chain. *Trends Plant Sci* 8:15–19.
4. Joliot P, Johnson GN, Joliot A (2006) Cyclic electron transfer around Photosystem I. *Photosystem I: The Light-Driven Plastocyanin:Ferredoxin Oxidoreductase*, ed Golbeck JH (Springer, Berlin), pp 639–656.
5. Johnson GN (2011) Physiology of PSI cyclic electron transport in higher plants. *Biochim Biophys Acta* 1807:384–389.
6. Albertsson PA (2001) A quantitative model of the domain structure of the photosynthetic membrane. *Trends Plant Sci* 6:349–358.
7. Albertsson PA (1995) The structure and function of the chloroplast photosynthetic membrane: A model for the domain organization. *Photosynth Res* 46:141–149.
8. Joliot P, Lavergne J, Beal D (1992) Plastoquinone compartmentation in chloroplasts. 1. Evidence for domains with different rates of photo-reduction. *Biochim Biophys Acta* 1101:1–12.
9. Lavergne J, Bouchaud JP, Joliot P (1992) Plastoquinone compartmentation in chloroplasts. 2. Theoretical aspects. *Biochim Biophys Acta* 1101:13–22.
10. Kirchhoff H, Horstmann S, Weis E (2000) Control of the photosynthetic electron transport by PQ diffusion microdomains in thylakoids of higher plants. *Biochim Biophys Acta* 1459:148–168.
11. Seelert H, et al. (2000) Structural biology. Proton-powered turbine of a plant motor. *Nature* 405:418–419.
12. Joliot P, Joliot A (2008) Quantification of the electrochemical proton gradient and activation of ATP synthase in leaves. *Biochim Biophys Acta* 1777:676–683.
13. Heber U, Walker D (1992) Concerning a dual function of coupled cyclic electron transport in leaves. *Plant Physiol* 100:1621–1626.
14. Clarke JE, Johnson GN (2001) In vivo temperature dependence of cyclic and pseudocyclic electron transport in barley. *Planta* 212:808–816.
15. Makino A, Miyake C, Yokota A (2002) Physiological functions of the water-water cycle (Mehler reaction) and the cyclic electron flow around PSI in rice leaves. *Plant Cell Physiol* 43:1017–1026.
16. Harbinson J, Woodward FI (1987) The use of light-induced absorbency changes at 820 nm to monitor the oxidation-state of P-700 in leaves. *Plant Cell Environ* 10:131–140.
17. Harbinson J, Foyer CH (1991) Relationships between the efficiencies of photosystems I and II and stromal redox state in CO₂-free air: Evidence for cyclic electron flow in vivo. *Plant Physiol* 97:41–49.
18. Ott T, Clarke J, Birks K, Johnson G (1999) Regulation of the photosynthetic electron transport chain. *Planta* 209:250–258.
19. Foyer C, Furbank R, Harbinson J, Horton P (1990) The mechanisms contributing to photosynthetic control of electron-transport by carbon assimilation in leaves. *Photosynth Res* 25:83–100.
20. Johnson GN (2003) Thiol regulation of the thylakoid electron transport chain—a missing link in the regulation of photosynthesis? *Biochemistry* 42:3040–3044.
21. Hald S, Nandha B, Gallois P, Johnson GN (2008) Feedback regulation of photosynthetic electron transport by NADP(H) redox poise. *Biochim Biophys Acta* 1777:433–440.
22. Sazanov LA, Burrows PA, Nixon PJ (1998) The plastid ndh genes code for an NADH-specific dehydrogenase: Isolation of a complex I analogue from pea thylakoid membranes. *Proc Natl Acad Sci USA* 95:1319–1324.
23. Joliot P, Joliot A (2002) Cyclic electron transfer in plant leaf. *Proc Natl Acad Sci USA* 99:10209–10214.
24. Joliot P, Béal D, Joliot A (2004) Cyclic electron flow under saturating excitation of dark-adapted Arabidopsis leaves. *Biochim Biophys Acta* 1656:166–176.
25. Cleland RE, Bendall DS (1992) Photosystem-I cyclic electron-transport: measurement of ferredoxin-plastoquinone reductase-activity. *Photosynth Res* 34:409–418.
26. Moss DA, Bendall DS (1984) Cyclic electron-transport in chloroplasts: The Q-cycle and the site of action of antimycin. *Biochim Biophys Acta* 767:389–395.
27. Mitchell P (1975) The protonmotive Q cycle: A general formulation. *FEBS Lett* 59:137–139.
28. Crofts AR, Meinhardt SW, Jones KR, Snozzi M (1983) The role of the quinone pool in the cyclic electron-transfer chain of *Rhodospseudomonas spaeroides*. A modified Q-cycle mechanism. *Biochim Biophys Acta* 723:202–218.
29. Clark RD, Hawkesford MJ, Coughlan SJ, Bennett J, Hind G (1984) Association of ferredoxin NADP⁺ oxidoreductase with the chloroplast cytochrome b-f complex. *FEBS Lett* 174:137–142.
30. Zhang HM, Whitelegge JP, Cramer WA (2001) Ferredoxin:NADP⁺ oxidoreductase is a subunit of the chloroplast cytochrome b6f complex. *J Biol Chem* 276:38159–38165.
31. Wollman F-A, Bulté L (1989) Toward an understanding of the physiological role of state transitions. *Photoconversion Processes for Energy and Chemicals*, eds Hall DO, Grassi G (Elsevier, Amsterdam), pp 198–207.
32. Iwai M, et al. (2010) Isolation of the elusive supercomplex that drives cyclic electron flow in photosynthesis. *Nature* 464:1210–1213.
33. Munekage Y, et al. (2002) PGR5 is involved in cyclic electron flow around photosystem I and is essential for photoprotection in Arabidopsis. *Cell* 110:361–371.
34. DalCorso G, et al. (2008) A complex containing PGR1 and PGR5 is involved in the switch between linear and cyclic electron flow in Arabidopsis. *Cell* 132:273–285.
35. Nandha B, Finazzi G, Joliot P, Hald S, Johnson GN (2007) The role of PGR5 in the redox poising of photosynthetic electron transport. *Biochim Biophys Acta* 1762:1252–1259.
36. Walters RG, Horton P (1991) Resolution of components of nonphotochemical chlorophyll fluorescence quenching in barley leaves. *Photosynth Res* 27:121–133.
37. Maxwell K, Johnson GN (2000) Chlorophyll fluorescence—a practical guide. *J Exp Bot* 51:659–668.
38. Johnson MP, Ruban AV (2010) Arabidopsis plants lacking PsbS protein possess photoprotective energy dissipation. *Plant J* 61:283–289.
39. Joliot P, Joliot A (2006) Cyclic electron flow in C3 plants. *Biochim Biophys Acta* 1757:362–368.
40. Joliot P, Joliot A (2005) Quantification of cyclic and linear flows in plants. *Proc Natl Acad Sci USA* 102:4913–4918.
41. Delosme R (1967) Study of the induction of fluorescence in green algae and chloroplasts at the onset of an intense illumination (Translated from French). *Biochim Biophys Acta* 143:108.
42. Strasser RJ, Srivastava A, Govindjee (1995) Polyphasic chlorophyll-a fluorescence transient in plants and cyanobacteria. *Photochem Photobiol* 61:32–42.
43. Hajirezaei MR, et al. (2002) Small changes in the activity of chloroplastic NADP (+)-dependent ferredoxin oxidoreductase lead to impaired plant growth and restrict photosynthetic activity of transgenic tobacco plants. *Plant J* 29:281–293.
44. Harbinson J, Hedley CL (1989) The kinetics of P-700⁺ reduction in leaves: A novel in situ probe of thylakoid functioning. *Plant Cell Environ* 12:357–369.
45. Genty B, Briantais J-M, Baker NR (1989) The relationship between quantum yield of photosynthetic electron transport and quenching of chlorophyll fluorescence. *Biochim Biophys Acta* 990:87–92.
46. Bilger W, Björkman O (1990) Role of the xanthophyll cycle in photoprotection elucidated by measurements of light-induced absorbance changes, fluorescence and photosynthesis in leaves of *Hedera canariensis*. *Photosynth Res* 25:173–185.